Research Article

생체흡수성 마그네슘의 생체 부식이 매식 환경에 미치는 영향

김유경, 김서영, 이민호, 장용석*

전북대학교 치과대학 치과생체재료학교실, 생체흡수성소재연구소

Effects of biocorrosion of biodegradable magnesium on the implantation environment

Yu-Kyoung Kim, Seo-Young Kim, Min-Ho Lee, Yong-Seok Jang*

Department of Dental Biomaterials, Institute of Biodegradable Materials,
School of Dentistry, Jeonbuk National University, Jeonju, Republic of Korea

생체흡수성 마그네슘 금속재료는 체내에서의 생 분해 특성과 생물학적 적합성으로 인해 치과 및 정형외과 분야에서 임시 임플란트로서 주목받고 있다. 본 연구는 마그네슘 금속의 부식과 이온 방출이 세포 및 조직 환경에 미치는 영향을 *in vitro* 및 *in vivo*를 통해 종합적으로 분석하였다. 배양액 내 마그네슘 이온 농도와 pH 변화가 골아 세포의 증식과 분화, 그리고 대식세포의 염증 반응에 미치는 영향을 평가하였다. 그 결과, 약 알칼리성 환경(pH 8~8.5)에서 쥐 골아 세포의 alkaline phosphatase 활성이 증가하고 세포 생존율이 높게 나타났으나, 골아 세포와 대식세포의 공동 배양 환경에서는 pH 7 이외의 조건에서 염증성 사이토카인(TNF-α 및 IL-1β) 분비와 파골 세포로의 분화가 촉진되었다. 이는 마그네슘 부식으로 인한 국소 알칼리화가 염증과 골 흡수 경로를 자극할 수 있음을 시사한다. *In vivo* 평가는 쥐의 피부 및 근육 내 마그네슘 삽입 후 초기 부식 과정에서 가스 형성과 주변 조직의 변화를 관찰하였다. 근육 조직 내에서는 매식 초기 3주 동안 많은 양의 가스가 체내 흡수되지 않고 존재하였으나 6주 이후 점차 감소하였으며, 12주 후에는 대부분의 가스가 사라졌다. 반면, 피부 내 조직에서는 더 빠른 가스 흡수와 조직 회복이 이루어졌다. 부식으로 인한 가스 형성과 조직 변화는 염증 반응과 세포 간의 상호작용을 촉진하여, 장기적으로 마그네슘 임플란트의 안정성에 영향을 미칠 수 있다.

색인단어 : 마그네슘, 생분해능, 세포 환경모사

Yu-Kyoung Kim (ORCID: 0000-0002-7081-2907)
Seo-Young Kim (ORCID: 0000-0003-3271-3307)
Min-Ho Lee (ORCID: 0000-0001-6142-4876)

*Correspondence: Yong-Seok Jang (ORCID: 0000-0002-2757-232X)
567, Baekje-daero, Deokjin-gu, Jeonju 54896, Republic of Korea
Affiliation: Department of Dental Biomaterials, Institute of Biodegradable Materials, School of Dentistry, Jeonbuk National University, Jeonju, Republic of Korea
Tel: +82-63-270-4041
E-mail: yjang@jbnu.ac.kr

Introduction

Magnesium is a biologically essential nutrient that contributes to bone and mineral homeostasis (1). Magnesium, as a biodegradable metal material including the recent dental field, has been the subject of many recent studies: alloying for magnesium implants for biomaterials (2, 3), post-treatment to improve mechanical strength (4), and surface treatment to improve corrosion resistance (5, 6). In particular, fixed implant screws or temporary implants (7) and membranes for sinus lift procedures (8) are being studied for dental purposes. The most important thing in dental implants is initial stability and promotion of bone regeneration. Magnesium promotes bone formation through ion release and has the potential to help bone recovery through interaction with surrounding tissues during the decomposition process in the body (9).

Magnesium metal applied to bone loss and fracture sites has many failure factors in human applications, despite many efforts, such as low mechanical properties (lower strength and fatigue limit than existing metal and ceramic materials), rapid decomposition, inflammatory response of surrounding tissues and bone absorption due to decomposition, and gaps with surrounding tissues due to hydrogen gas formation. Therefore, recently, biode- gradable metals are being used in mini-screws, vascular stents, bone guide regeneration, etc., which are relatively small in size or do not receive high loads. In past studies, the failure factors of implanted magnesium were reported to be increased pH between the material and tissue, gas gap formation, and concentration of magnesium ions (10), but it did not provide an accurate guideline on which factors act as problems in the body, and there is no specialized standard that can simulate the absorption mechanism of metallic biodegradable materials in the body. In terms of alloying to complement the short- comings of magnesium implants, the mechanical strength can be increased by adding non-biotoxic ions (Mg, Zn, Ca, etc.), but the addition of rare earth elements for effective property improvement raises questions about biosafety (11, 12). Thus, prior to developing magnesium materials for use in various fields, it is important to find out the exact cause of the problems that metallic magnesium causes to the human body when dissolved.

In vitro evaluation of magnesium has mainly been performed by assessing pH changes, mass changes, gas formation, and direct and indirect cytotoxicity after deposition in similar body fluids(13). When osteoblasts are cultured directly on magnesium, they exhibit low cell compatibility due to complex causes such as cell detachment due to gas bubble formation, cell death due to rapid increases in pH, and increased magnesium ion release, making it difficult to achieve cell proliferation and differentiation through long-term culture. Therefore, we use an indirect method of growing cells in a solution environment where magnesium is dissolved in the cell medium, referring to ISO 10993-Biological evaluation of medical devices (14) and ASTM F3268-18a -New Guide for *In-Vitro* Degradation Testing of Absorbable Metals (15).

These standards guide the setting of the amount of medium to be extracted, temperature, and extraction time according to the thickness and volume of bioactive and inert metal specimens, but these have limitations in biocompatibility tests of biodegradable magnesium, which have various variables mentioned above. Although the negative effects of increased pH on bone cells when magnesium is decomposed in the body have been reported, studies on cytotoxicity according to pH changes have been limited. This study analyzed the exact mechanism by which magnesium decomposition affects the inflammatory response by quantitatively evaluating the expression of inflammatory cytokines (TNF-α, IL-1β) using RAW 264.7 macrophages under various environ- ments from PH 5.5 to 11.5. In an original study, the effects of magnesium on osteoclast activation and bone

resorption were analyzed through co-culture of osteoblasts (MC3T3-E1) and macrophages (RAW 264.7). Bone is regenerated to maintain strength and mineral homeostasis. In the process, osteoclasts remove old bone cells and osteoblasts form and differentiate new bone. However, excessive osteoclast activity can inhibit bone regeneration and cause bone resorption (16).

The authors of this study have studied magnesium implantation in bone defects for many years and found that the amount of gas formed around the same specimen varied, and there were variables depending on the amount of body fluid or blood exposure of the tissue around the implant (13, 17). In addition, it has been known in previous studies that magnesium metal for use as implants releases magnesium ions (Mg^{2+}) into the body, which are absorbed by bone cells and used for the formation of new bone tissue (18), but research on the absorption mechanism for tissues in contact with tissues is lacking. This is because there are many variables in reproducing gas formation and differentiation processes of tissue cells under the same conditions in muscle and adipose tissues. Based on this, we intend to examine the problems that occur during magnesium implantation in vivo, the gas pockets caused by rapid magnesium corrosion, and the resulting changes in adjacent tissues.

Materials and Methods

1. Materials Preparation

A pure Mg plate (Mg 99.9%, Goodfellow, Cheshire, England) was cut as $10 \times 20 \times 2T$ (mm), and was sequentially ground using 800 to 2000 grit silicon carbide papers. All samples were washed with ethanol and stored in a 37 ℃ dry oven.

2. Osteoblast viability according to the amount of Mg ion

To evaluate the effect of Mg ions on osteoblasts, the samples were extracted at 1.25 cm^2/mL in α-MEM at 36 ℃ for 48 h according to ISO 10993-12 (14). The extracts were filtered through 0.2 μm and prepared at concentrations ranging from 10 to 100% with α-MEM. To evaluate only the ionic influence of magnesium, the pH was adjusted to 7.4 (added HCl). The quantitative analysis of Mg, Ca and P in the extract solution was performed 5 times by using Inductively Coupled Plasma Mass Spectrometry (ICP-MS, Agilent 7500a, Agilent Technologies, CA, USA). Statistical significance of all data was analyzed by Mann-Whitney Test (P value < 0.05 was considered significant).

Osteoblast cells MC3T3-E1 was purchased from ATCC (American Type Culture Collection). 10% fetal bovine (FBS, Gibco Co., Jenks, USA), 500 unit/mL of penicillin (Gibco Co., Jenks, USA), and 500 unit/mL of streptomycin (Gibco Co., Jenks, USA) were added to α-MEM (Gibco Co., Jenks, USA) to prepare the culture media. The cells were incubated in cell culture plates at 1.5×10^4 cells/well in 24 well and incubation was carried out at 37 ℃ in an atmosphere containing 5 vol.% CO_2 for 6 hours to allow cell attachment. And then, the culture media was removed and replaced for eluate solution. Cellular cytotoxicity was determined using the cell proliferation assay as a standard water-soluble tetrazolium salt (WST-8 kit) (96992, Sigma, St. Louis, USA) for colorimetric analyses after incubation for 2 and 4 days. The formazan dye was subsequently measured using a microplate spectrophotometer (EMax, Molecular Devices, San Jose, USA) at a wavelength of 490 nm. Also, the cultured cell was stained with 0.3% crystal violet for observations of the cell morphology by optical microscopy (DM2500, Leica, Tokyo, Japan).

For alkaline phosphatase (ALP) activity, the cultured cell after 10 days, the substrate solution [0.2M Tris-HCl buffer with p-nitro-phenyl phosphate (pNPP)] was added to each well and react at 37 ℃ for 60 minutes by using an ALP assay kit (MK301, Takara, Kusatsu, Japan). The absorbance was measured at 405 nm using a microplate spectrophotometer.

For Alizarin Red staining, the cultured cell after 15 days fixed with 3% formaldehyde, and stained with 40 mM Alizarin Red S (Sigma, St. Louis, USA) (pH 4.2) for 15 min at room temperature. Images of the cell morphology were observed by optical microscopy. 10% Chloride monohydrate was added and incubated for 15 min with shaking. The absorbance of the supernatant was measured at 570 nm using a microplate spectrophotometer.

3. Osteoblast viability according to the pH variation

Based on the results of '2. Osteoblast viability according to the amount of Mg ion', the 40% dilution group of magnesium extract was selected, and cell viability according to pH change was observed. The medium was prepared by adjusting the pH to 5.5 to 11.5 with 1N HCl and 1M NaOH. Osteoblast cells MC3T3-E1 were cultured according to the above procedure, and WST-8 was evaluated after 2 and 5 days, and ALP was analyzed after 10 days of culture (same protocol as 2).

4. The inflammatory cytokines in macrophage RAW 264.7

Based on the results of 2, the expression of inflammatory cytokines in the Mg 40% extract at pH 6 to 10 was measured. The RAW 264.7 macrophage cell line was obtained from the Korea Cell Line Bank (Seoul, Korea). 4.0×10^5 cells were seeded in a 12 microwell plate using D-MEM (with 10% FBS) medium and cultured for 6 hours. Afterwards, the medium was removed and replaced with D-MEM (with 0.5% FBS) and cultured for 18 hours. Each

eluate was replaced with D-MEM (with 0.5% FBS), and LPS 0.5 μg/mL was added to each well and cultured for 7 days. The control group was D-MEM (with 0.5% FBS), D-MEM (with 10% FBS), D-MEM (with 0.5% FBS) add LPS 0.5 μg/mL. TNF-α and IL-1β were measured using TNF-α and IL-1β ELISA kits (BMS607-3 and BMS6002, Thermo fisher, Waltham, USA) using the supernatant after centrifugation (12,000 rpm, 3 min) of the cultured media. The absorbance of the supernatant was measured at 450 nm using a microplate spectrophotometer. The macrophage cell morphology was stained with 0.3% crystal violet by optical microscopy.

5. Osteoclast activity

MC3T3-E1 cells (5×10^4 cells/well) and RAW 264.7 murine monocytic macrophage cells (8×10^4 cells/well) were co-cultured at in 12 wells in α-MEM. Incubation was carried out at 37 ℃ in an atmosphere containing 5 vol% CO_2 for 20 h. Each extract was replaced with α-MEM and cultured in a humidified atmosphere with 5% CO_2 at 37 ℃ for 8 days. To assess the formation and activity of osteoclasts, the substrate solution (0.5 M sodium acetate with pNPP) and 0.5 M sodium tartrate were added to each well and made to react at 37 ℃ for 60 min using an TRACP assay kit (MK301, Takara, Kusatsu, Japan). The stop solution (0.5 N NaOH) was added for color formation, and the absorbance was measured at 405 nm using a microplate spectrophotometer. The osteoclast cells were stained with a tartrate-resistant acid phosphatase (TRAP) staining kit (B-Bridge International, Inc., Cupertino, USA) and were observed by optical microscopy.

6. *In vivo*

The animal study was according to the Declaration of Helsinki and was approved by the Institutional Animal Care and Use Committee of the Jeonbuk National

University Laboratory Animal Center (CBNU 2020-096). Mg foil (Mg 99.9%, As rolled, Goodfellow, Cheshire, England) was cut as 2×4×0.1 (mm), and sterilized with ethylene oxide gas for 8h at 40 ℃ and 1.7 bar of atmospheric pressure. Mg foils were used for implantation in twelve male Sprague Dawley rats (8-week-old, weight: 260−280 g) as Figure 1(a). Samples were inserted into the subdermal site of the back [Figure 1(b)] and into the buttock intermuscular site [Figure 1(c)) of the rats. In the control group, the incision was made at the same location as the sample group and the wound was sutured. A total of four samples were inserted, two on each side of the spine per rat. Three rats were sacrificed every 3, 6, 9 and 12 weeks to obtain surrounding tissues. The shape of the samples and surrounding gas formation were quantified using micro-CT installed in the Center for University-wide Research Facilities (CURF) at Jeonbuk National University.

7. Statistical analysis

The Mann-Whitney U test, using SPSS software, version 12.0K (SPSS, Inc., Chicago, IL, USA), was applied to compare the mechanical properties, with significance determined at a 0.05 level. Data marked with an asterisk indicate that there is no significant difference between groups.

Results

To observe the effect of magnesium metal ions on cells *in vitro*, the ions were eluted into cell medium according to ISO standards, and the amounts of Mg, Ca, and P were measured by ICP. (Figure 2 and Table 1). α-MEM cell medium basically contains (18.74±0.23) ppm of Mg, (70.9±0.99) of Ca, and (36.72±0.59) ppm of P. After magnesium dissolution, Mg increased significantly to (115.39±2.49) ppm, but the amounts of Ca and P decreased. As a result of measuring the amount of ions concentration in the medium after culturing cells for 7 days, the increase rates of Mg, Ca, and P ions in α-MEM and the eluate all showed an increasing trend, ranging from 23 to 34%. The group in which the magnesium solution was diluted 30% showed an increase of 71.09% for Mg ions, and 20.8 and 31.7% for Ca and P, respectively. However, in the group in which the magnesium solution was diluted more than 70%, the ion increase rate was within 20%. Considering the moisture evaporating during cell culture, it shows that the ion changes in the group in which the magnesium solution was diluted more than 70% was low. Statistically significant differences were observed in all groups.
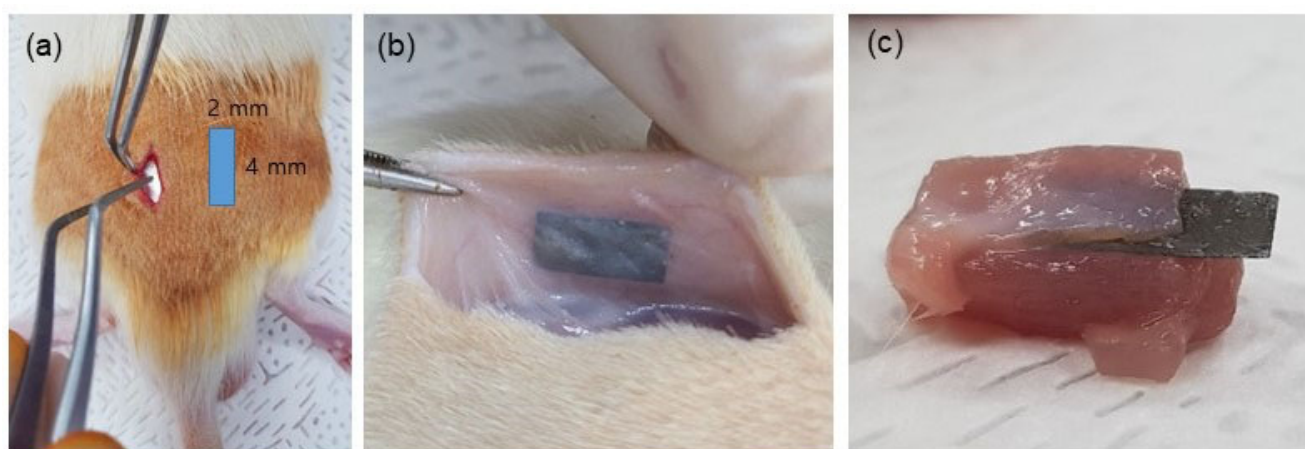

Figure 1. (a) Location of implantation of magnesium foil in rat, (b) subdermal and (c) intermuscular regions
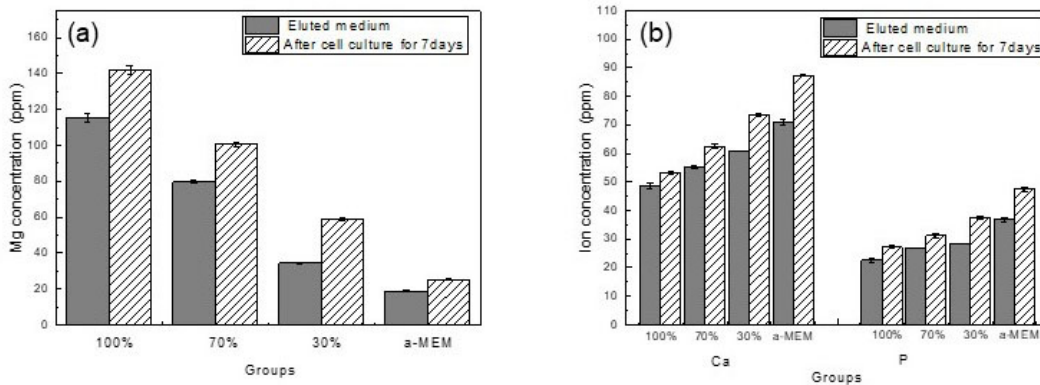
Figure 2. After adding magnesium to the medium, the amount of magnesium ions (a) and the amount of Ca and P ions (b) according to the medium dilution ratio

Table 1. Ion concentration of Mg eluate

Group\Ion concentration (ppm)		Mg	Ca	P
Eluted medium	100% eluate	115.39	48.64	22.54
	α-MEM	18.74	70.9	36.72
After cell culture for 7 days	100% eluate	142.10	53.24	27.12
	α-MEM	25.27	87.29	47.58

When magnesium is dissolved in the medium, the pH increases rapidly, but in this study, the pH was maintained at 7.4 and the amount of magnesium ions was changed to determine only the effects of Mg, Ca, and P ions on the bioactivity of osteoblasts. As a result of WST-8 assay Figure 3(a), the 100% extraction medium containing (115.39±2.49) ppm magnesium showed the lowest cell viability, and cell viability increased rapidly after the magnesium ion amount was reduced by more than 50%. There was no significant difference in the group diluted to less than 40%, and the cell viability of all groups was lower than the α-MEM medium. A result of crystal violet staining as Figure 3(d), there was no difference in the number of cells between the control group and the 30% extraction group, but the shape of the osteoblast filopodia became thinner and longer as the amount of magnesium

increased, and it was confirmed that the number of viable cells decreased rapidly at 50% or more. The ALP results [Figure 3(b)) showed a similar pattern to the WST results, and the groups diluted to less than 20% showed no significant difference compared to the control. In particular, the results of the alizarin red assay evaluating the amount of Ca [Figure 3(c and e)] showed that the groups diluted to less than 40% and less than 20% showed no significant difference, and the group diluted to less than 10% showed the highest value, and the cell nucleus and cytoplasm were stained.

While maintaining the pH at 7.4, the amount of magnesium ions was varied to observe cell proliferation and differentiation. As a result, it was determined that cytotoxicity was low when the dilution amount was within 40% (within approximately 76 ppm of Mg). After fixing
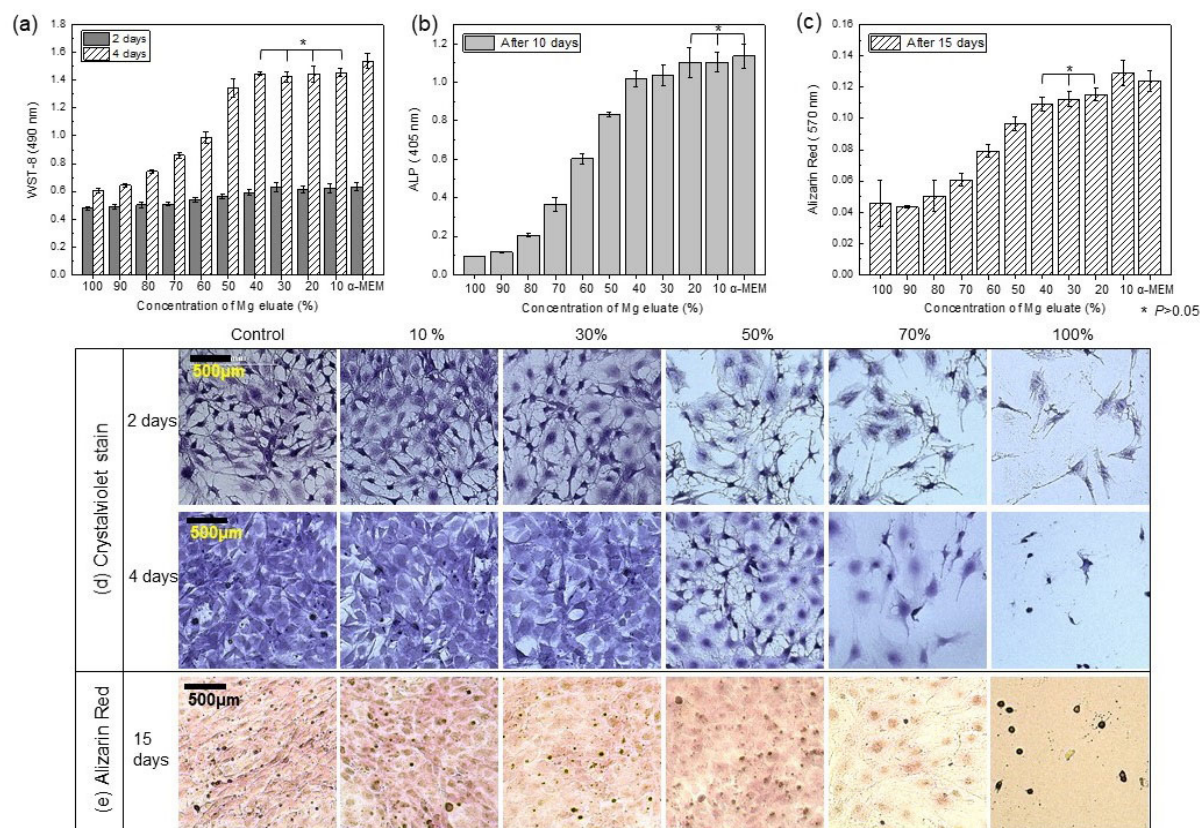
Figure 3. WST-8 assay (a), ALP (b), Alizarin red assay (c and e), and crystal violet staining (d) of rat osteoblasts (MC3T3-E1) according to the concentration of Mg elute from media

the magnesium content at 40% and adjusting the pH, the cytocompatibility was evaluated. As a result, Figure 4(a) showed that cell proliferation was the highest at pH 8 to 8.5. In particular, compared to the control group, pH 7.5 showed an 89% survival rate, while pH 8 to 8.5 showed a survival rate of over 98%. The ALP results 10 days later showed high cell differentiation at the level of the control group without a significant difference in the pH 7 to 8.5 range.

To determine whether the cell growth environment is affected by pH, the results of the inflammatory response evaluation using M1 (Pro-inflammatory macrophages) macrophage cells (Figure 5A and B) showed that the TNF-α factor showed a suppressed function at pH 7 to 9 compared to the positive group [Figure 5A, (f)], and and the other groups showed increased inflammation

levels. IL-1β was suppressed at pH 7-8, and inflammatory factors were induced at pH 8 or higher and pH 6. As for the changes in cell morphology, as shown in the crystal violet staining results in Figure 5C, the negative control group that was not stimulated [Figure 5C.(h)] showed a typical round shape of macrophages, and macrophage deformation - formation of filopodia - could be seen due to the lack of FBS in the medium [Figure 5C.(g)]. Macrophages stimulated by LPS treatment showed not only cell deformation but also a decrease in cells [Figure 5C.(f)], but did not show cytotoxicity at pH 8 and 9. In acidic or alkaline conditions, the number of viable cells decreased and filopodia expanded.

As a result of the co-culture interaction between osteoblasts and macrophages, which induced macrophages to become osteoclasts, Figure 6 shows that TRACP
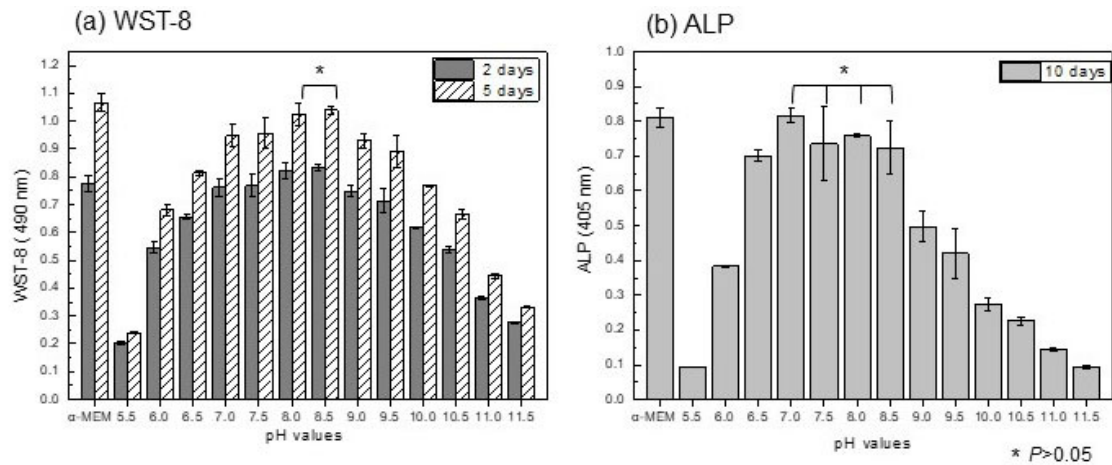
Figure 4. WST-8 assay (a) and ALP (b) evaluation of MC3T3-E1 cell by changing the pH of the medium while fixing the Mg dissolution dilution amount to 40%
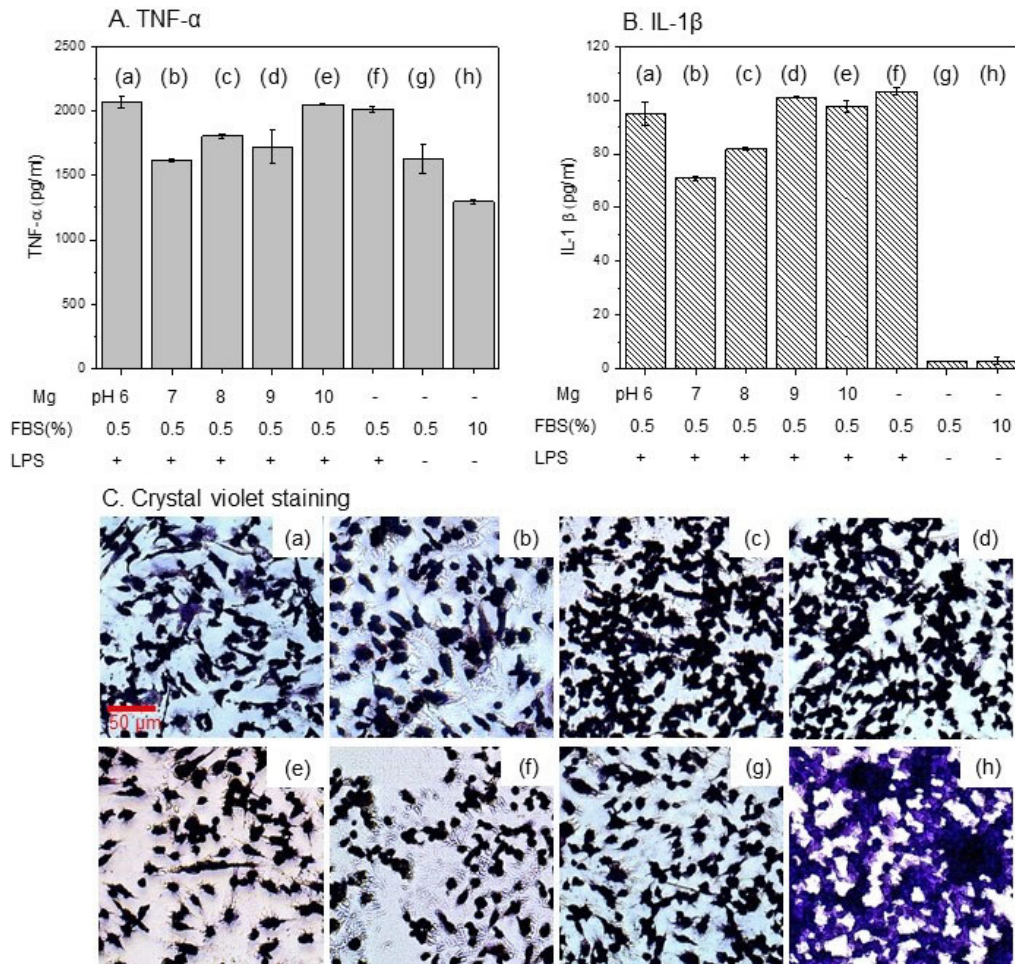

Figure 5. A. Inflammation levels from TNF-α, B. IL-1β factor and C. crystal violet staining of co-cultured MC3T3-E1 cell and RAW 264.7 macrophage cell by changing the pH of the medium : (a) pH 6, (b) pH7 , (c) pH 8, (d) pH 9, (e) pH10, (f) media with LPS treatment for positive control, (g) media with 0.5% FBS and (h) media with10 % FBS for negative control
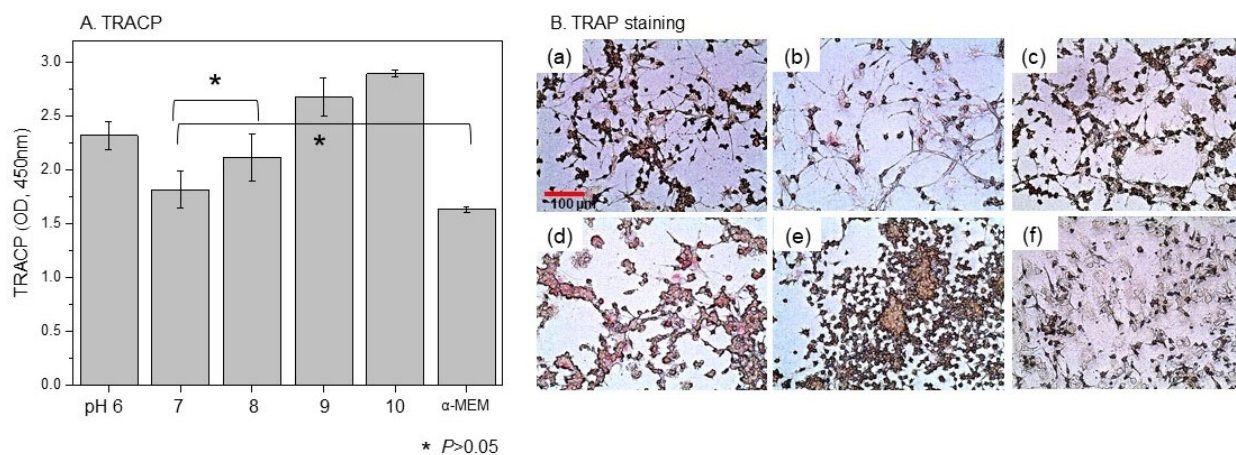
Figure 6. A. TRACP and B. TRAP assay for differentiation into osteoclasts in a co-culture environment with MC3T3-E1 cells and RAW 264.7 macrophage cells

showed the lowest value at pH 7 and showed no significant difference from pH 8, and no difference from the negative control group. As a result of TRAP staining to observe cell transformation (Figure 6B), the negative control group (f) showed a stable distribution of osteoblasts and macrophages, but in an environment of pH 8 or higher, osteoblasts decreased while the number of macrophages increased rapidly (d and e). Even in the pH 7 group [Figure 6B(b)] where there was no quantitative increase in macrophages, the cell filopodia of osteoblasts were elongated and showed a decrease.

To investigate the gas formation and absorption of magnesium, and its solubility in tissue, magnesium foil was inserted between the intermuscular and subdermal region of the back of rats and monitored for 12 weeks (Figure 7). The gas pockets formed from magnesium in rat tissue (Figure 7A) increased rapidly in the intermuscular region until 6 weeks and were gradually absorbed into the tissue until 12 weeks. In the case of subdermal magnesium, the amount of initially formed magnesium gas was greater than that in the intermuscular region (3-week result), but the absorption rate was faster and the amount of gas tended to decrease continuously. In both locations, the gas pockets had virtually disappeared

after 12 weeks, and the rate of degradation of the magnesium specimens had decreased by 50% by 3 weeks and then gradually decreased in volume. In particular, in the case of intermuscular implantation, the initial magnesium corrosion rate was relatively slow, but it was similar in the long term. Micro CT measurement results (Figure 7C) showed that the central part vulnerable to stress was damaged due to the dissolution of the magnesium specimen at both locations 9 weeks after implantation.

Figure 8 shows the tissue changes over time observed using HE stain after implantation of magnesium under the intermuscular and subdermal layers. The control group maintained normal tissue after 6 weeks despite the incision. 3 weeks after implantation into the intermuscular cavity, purple-stained multi-nuclei were intensively formed around the Mg plate, and macrophages were dispersed throughout the muscle tissue after 6 weeks. After 9 weeks, macrophages were concentrated only around the Mg, and the surrounding tissues were recovering to normal cells. On the other hand, purple macrophage concentration was observed 6 weeks after Mg implantation under the subdermal layer, and was not observed after 9 weeks, showing normal skin tissue.
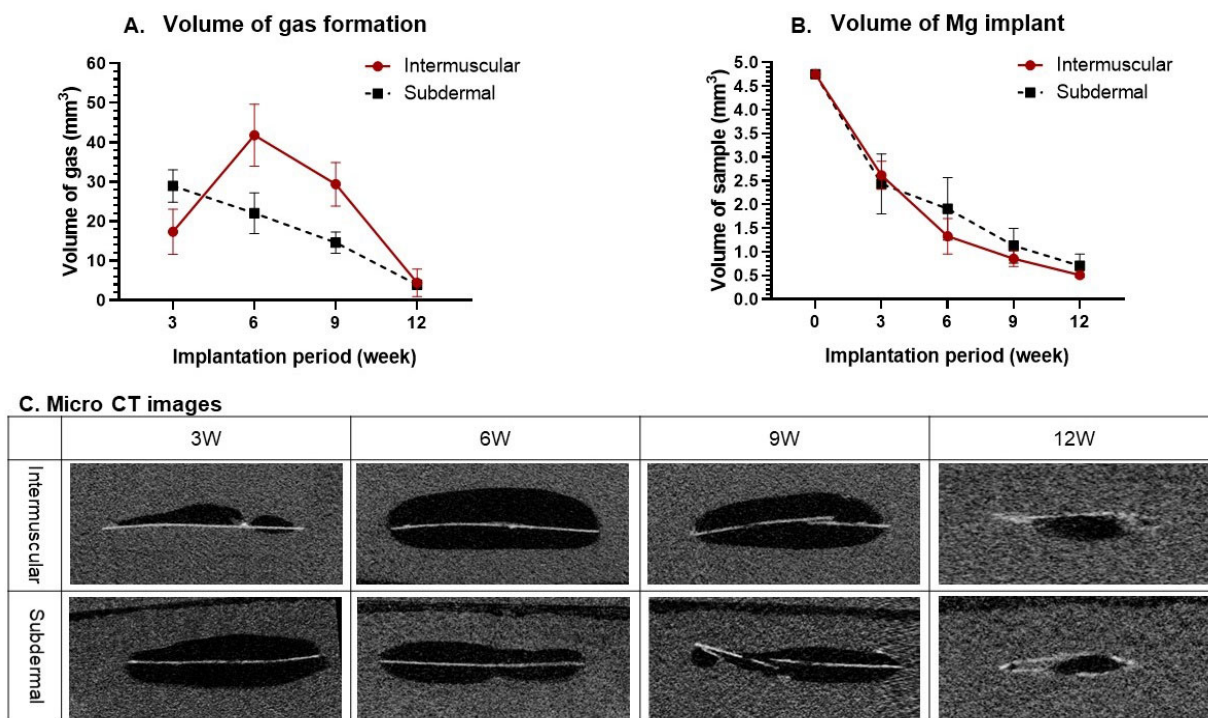
Figure 7. A. The gas formation, B. absorption volume of magnesium, and C. Micro CT images from the intermuscular and subdermal of rat
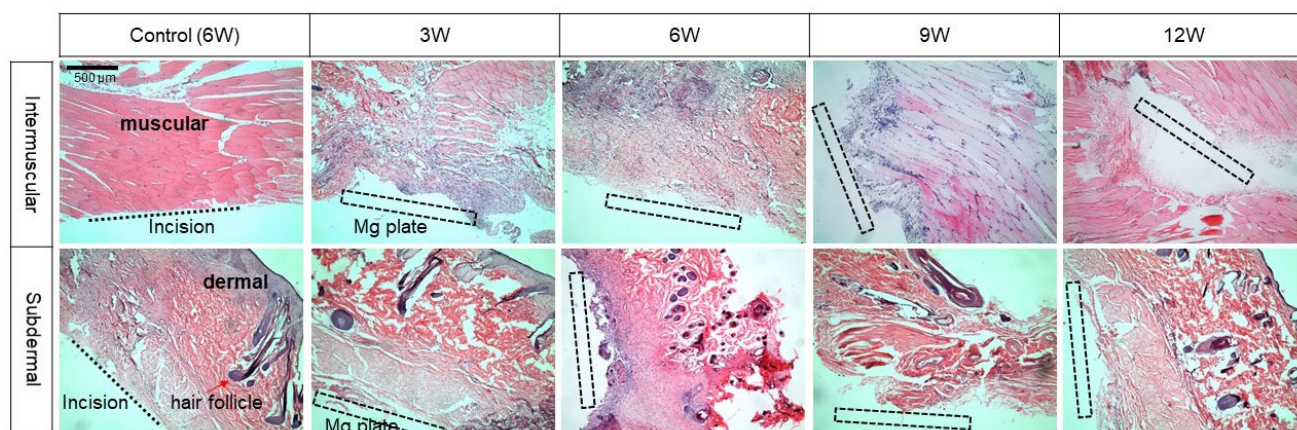

Figure 8. Observation of tissue changes around the implant in the intermuscular and subdermal areas using HE staining

Discussion

This study provides basic data to overcome the high decomposition rate, local corrosion, and mechanical strength limitations of magnesium metal as a bioabsorbable material including dentistry, and to increase the possibility of applying magnesium materials to the human body. According to the study, magnesium implants are reported to release about 10-30 mg/cm² of magnesium ions per day through the corrosion process in the body. This amount can vary greatly depending on the pH of the surrounding tissue, body fluid flow, and the corrosive

252

environment (e.g., bone marrow and blood flow). The only standard method for evaluating the cytotoxicity of magnesium biomaterials is to refer to ISO 10993-5 and ISO 10993-12. Accordingly, when magnesium is eluted and a cytotoxicity test is performed, the magnesium in the medium increases to (115.39 ± 2.49) ppm ion amount and the pH increases to 10. Although buffers (e.g., HEPES, bicarbonate) are added to the culture medium, the pH cannot be adjusted when the limit is reached, and the buffering capacity of the culture medium is limited in the cell culture environment. On the other hand, in the body tissue, the pH is quickly adjusted through the bicarbonate ion (HCO_3^-) in the blood and the protein buffer system, so cytotoxicity is minimized (19). These experimental limitations result in differences in the biocompatibility of magnesium implants *in vivo* and *in vivo*.

Accordingly, when magnesium was extracted and a cytotoxicity test was performed, the cell survival rate and differentiation in Figure 3(a) and (b) were significantly lower than those of the negative control group, so many studies were conducted in which the solution was diluted arbitrarily by a ratio of 2 to 10 times without any regulations (20, 21). In the results of this study, since a rapid decrease in survival was observed when the dilution rate was 50% in the proliferation of osteoblasts and cell differentiation according to ALP, a dilution of 40 to 50% compared to the ISO standard is suggested for the cytotoxicity test of the extract for treatment to increase the biocompatibility of magnesium metal.

After dissolving magnesium into the medium, Ca and P in the medium decreased. This is because magnesium is corroded and attached to the Mg surface as OH, Ca^{2+}, H_2PO_4 in the SBF reacted with magnesium (22), $Ca_{10}(PO)_6(OH)_2$, $Ca_3(PO_4)_2$, $Mg_3(PO_4)_2$, and $(Ca_{0.86}Mg_{0.14})_{10}(PO_4)_6(OH)_2$ (23). When the deficiency of P and Ca in the medium is more than 15%, hydroxyapatite formation is inhibited in the mineralization stage of osteoblasts.

Therefore, to support bone formation activities including alkaline phosphatase (ALP) activity and matrix mineralization, the calcium (Ca^{2+}) level is maintained at 1.8 mM (72.14 ppm) and the phosphate (Pi) concentration is maintained at approximately 1.5 mM (30.97 ppm) (24). The results of this study showed that after culturing osteoblasts for 10 days, ALP did not differ significantly from the control group in diluted medium of 20% or less, but after 15 days, Alizarin red detection was within the normal range only in diluted medium of 10% or less. This means that although there is no toxicity in cell proliferation within 4 days, a significant decrease in osteocytes is observed in long-term cell culture for bone mineralization evaluation, and thus the presence or absence of osteoblast toxicity cannot be determined by a simple numerical decrease in osteoblasts. Based on the WST results, the cell death was significantly high in the dissolution range (40% dilution concentration), and when only the pH of the medium was changed, positive cell differentiation and proliferation were observed at slightly alkaline (pH 8.5). According to past studies, when the pH of the medium was adjusted to slightly alkaline, cell proliferation increased as ALP (alkaline phosphatase) activity was increased in a slightly alkaline environment, and the extracellular matrix maturation and mineralization stages were also promoted (25). Also, concentrations below 10 mM were beneficial for cell growth, while pH 8.5, consideration of sediment and concentration of corrosion products had a negative effect on osteoclast precursor cell counts and mature osteoclast function (26).

However, in co-culture assays of osteoblasts and macrophages, we found that secretion of IL-1β increased even in pH 8 medium. TNF-α and IL-1β are representative inflammatory cytokines, indicating that inflammation is activated in the immune response (27). But in certain situations (when acting as a regulator of the immune response, removing pathogens or cells that induce inflammatory responses, or interacting with NFR1

(promoting inflammation) and TNFR2 (promoting cell survival and tissue repair)), TNF-α may contribute to the suppression of inflammation. IL-1β's induction of inflammation serves as a major mechanism for macrophages to differentiate into osteoclasts via the RANKL-RANK pathway. In this study, TNF-α was suppressed in pH 8~9 media, but IL-1β was secreted and differentiation into osteoclasts was confirmed through TRAP, suggesting that IL-1β factor expression is more significant. These results suggest that local environmental changes or alkalinization due to magnesium corrosion may have stimulated inflammatory pathways (28).

In a co-culture environment where osteoblasts and macrophages coexist, when stimulated by specific substances, macrophages can differentiate into osteoclasts through the RANKL (Receptor Activator of Nuclear Factor κB Ligand)-RANK pathway and M-CSF signaling. An increase in magnesium ions and an abnormal pH range environment induce the expression of RANKL, which binds to RANK (Receptor activator of nuclear factor kappa-b) in macrophages or hematopoietic cell lineage precursor cells to induce osteoclast differentiation. The binding of RANKL and RANK forms an important signaling pathway that promotes differentiation into osteoclasts by activating transcription factors such as NF-κB and NFATc1 (29). That is, as a result of confirming the osteoclast marker enzyme through tartrate-resistant acid phosphatase (TRAP) staining in Figure 6, increased osteoclast differentiation was observed in environments above and below pH 7~8, and macrophages are generally small mononuclear cells that are round and relatively small in size. However, when they differentiate into osteoclasts, macrophages increase in size and their cell shape changes irregularly (Figure 5C). It then grows into a large multinucleated cell that changes into a flat shape that contacts the bone surface widely. This is because osteoclasts contact a large area on the bone surface and secrete acids and enzymes to break down the bone (30).

In this study, alkaline or acidic cell media are the main factors that cause macrophage proliferation, osteoclast differentiation, and osteoblast reduction. In terms of magnesium ion content in the cell culture environment, past studies have shown that magnesium extracts of less than 2 mM do not affect osteoclast proliferation and differentiation (31). Although there was no significant difference in the expression of osteoclasts in a pH 7 environment, the morphology of macrophages changed to multinucleated, so in the long term, excessive magnesium ions will not cause osteoblast toxicity but will induce osteoclasts. This study limited the evaluation of pH changes in the medium in an experimental setting and did not fully reflect the circulating body fluids and complex pH regulation mechanisms (e.g., the buffer system of blood) in the actual body environment. This may lead to differences in biocompatibility between *in vivo* and in vivo experiments. The focus was on relatively short-term observations (up to 15 days) in assessing cell proliferation and toxicity, and further discussion of long-term cellular and immune responses is needed.

In order to understand the dissolution of biodegradable magnesium metal and the release of ions into the body, the formed gas and the changes in the surrounding local tissues *in vivo* are also important perspectives. This study examined the phenomenon and problems of dissolved magnesium in the intermuscular and subdermal regions. When magnesium metal is inserted into the body, it dissolves and forms gas. In the intermuscular region, it rapidly increases up to 6 weeks and then decreases, while in the subdermal region, the gas formed in the initial 3 weeks gradually decreased over time. In previous my studies, the gas was mainly composed of H_2, CO and CO_2. The maximum gas volume formed was 5 days in *in vivo* studies and 7 days in intramuscular clinical studies (13). Muscle tissue has active blood flow and fluid exchange, but gas discharge from the implantation site may be relatively limited, resulting in an initial rapid gas

accumulation. Later, as the tissue heals, the rate of corrosion decreases and gas discharge is alleviated. Blood flow and fluid exchange are relatively limited within the subdermal layer, and the rate of gas formation is slow, but continues for a certain period of time and then slowly decreases (32, 33).

Although there was a difference in the amount of gas formation due to corrosion, there was no difference in the change in mass. In both the intermuscular and subdermal regions, corrosion of magnesium implants is promoted by contact with body fluids, and the chemical mechanism of the corrosion reaction does not show a significant difference because the composition of the body fluids in both environments is similar. Therefore, this does not directly affect the change in dissolved mass (10). At 6 to 9 weeks, when a gap between the magnesium and tissue is formed by a gas pocket, nucleation is concentrated at the incision site. The formation of small nuclei around the implant is mainly caused by the activation of macrophages or inflammatory cells (34). The implantation of magnesium implants into the inter-muscular and subdermal regions is an important factor to be confirmed for use as a dental temporary implant. It is usually used to maintain the function and position of the tooth after tooth extraction until the permanent implant is prepared. Therefore, according to this study, it can provide a stable implant because the recovery of intradermal tissue is faster than intramuscular. Also the corrosion rate control and local environment (pH, inflammatory response, etc.) management techniques proposed in the study will contribute to increasing the stability and healing rate of implants. Absorbable magnesium is expected to have a wide range of medical applications, including as bioabsorbable vascular stents for the treatment of esophageal and colonic strictures, as urethral stents, or as devices for the treatment of kidney stones, and as a bioactive metal to aid in nerve regeneration in psychiatric and neurosurgical settings, and as a temporary support device for the repair of damaged nerve tissue.

Conclusion

This study comprehensively examined the effects of the corrosion process and ion release of magnesium metal on cytotoxicity and bone-related cell activities. In particular, through experimental analysis of the effects of magnesium ion concentration and pH changes on the physiological responses of osteoblasts and macrophages, it was found that in a slightly alkaline pH environment where only osteoblasts were cultured, ALP activity increased and there was no cytotoxicity, but in a coculture environment of osteoblasts and macrophages, when the pH changed to an abnormal range, the secretion of inflammatory cytokines TNF-α and IL-1β increased and osteoclast differentiation was promoted. This suggests that alkalinization due to magnesium corrosion can stimulate inflammation and bone resorption pathways. Gas formation and changes in the cellular environment due to corrosion play an important role in the inflammatory response and osteoclast differentiation, which provides important basic data for increasing the possibility of applying magnesium materials to dental implants.

Acknowledgement

References

1. De Baaij JH, Hoenderop JG, Bindels RJ. Magnesium in man: implications for health and disease. Physiol Rev. 2015;95(1):1-46.

2. Liu C, Yang H, Wan P, Wang K, Tan L, Yang K. Study on biodegradation of the second phase Mg17Al12 in Mg–Al–Zn Alloys: *In vitro* experiment and thermodynamic calculation. Mater Sci Eng C.2014;35(0):1-7.

3. Park JP, Kim MG, Yoon US, Kim WJ. Microstructures and mechanical properties of Mg–Al–Zn–Ca alloys fabricated by high frequency electromagnetic casting method. J Mater Sci. 2009;44(1):47-54.

4. Ji JH, Park IS, Kim YK, Lee SJ, Bae TS, Lee MH. Influence of Heat Treatment on Biocorrosion and Hemocompatibility of Biodegradable Mg-35Zn-3Ca Alloy. Adv Mater Sci Eng.2015;2015:10.

5. Li LH, Narayanan T, Kim YK, Kong YM, Shin GS, Lyu SK. Coloring and corrosion resistance of pure Mg modified by micro-arc oxidation method. Int J Precis Eng Manuf. 2014;15(8):1625-30.

6. Kim YK, Yoon DJ, Shin Ch, Hee RM, Jang YS, Lee MH. Surface characteristics of anodized AZ91D with potassium permanganate in alkaline by various time. Adv Mater Res.2013;704:141-8.

7. Vujovic Ristic S, Mojsilović J, Stanisic D, Ognjanović I, Stevanovic M, Rosic G. Applications of Biodegradable Magnesium-Based Materials in Reconstructive Oral and Maxillofacial Surgery: A Review. Molecules. 2022;27:5529.

8. Elad A, Pul L, Rider P, Rogge S, Witte F, Tadić D. Resorbable magnesium metal membrane for sinus lift procedures: a case series. BMC Oral Health. 2023; 23(1):1006.

9. Herber V, Okutan B, Antonoglou G, N GS, Payer M. Bioresorbable Magnesium-Based Alloys as Novel Biomaterials in Oral Bone Regeneration: General Review and Clinical Perspectives. J Clin Med. 2021; 10(9):1842.

10. Rahman M, Dutta NK, Roy Choudhury N. Magnesium Alloys With Tunable Interfaces as Bone Implant Materials. Front. Bioeng. Biotechnol. 8:564.

11. Myrissa A, Braeuer S, Martinelli E, Willumeit-Römer R, Goessler W, Weinberg AM. Gadolinium accumulation in organs of Sprague–Dawley® rats after implantation of a biodegradable magnesium-gadolinium alloy. Acta Biomater.2017;48:521-9.

12. Willbold E, Gu X, Albert D, Kalla K, Bobe K, Brauneis M, et al. Effect of the addition of low rare earth elements (lanthanum, neodymium, cerium) on the biodegradation and biocompatibility of magnesium. Acta Biomater.2015;11(1):554-62.

13. Kim YK, Lee KB, Kim SY, Bode K, Jang YS, Kwon TY, et al. Gas formation and biological effects of biodegradable magnesium in a preclinical and clinical observation. Sci Technol Adv Mater. 2018;19(1): 324-35.

14. Standardization IOf. ISO 10993, Biological Evaluation of Medical Devices-Part 12: Sample preparation and reference materials. ISO. 2017.

15. International A. New guide for in-vitro degradation testing of absorbable metals. ASTM Int. 2015.

16. Clarke B. Normal bone anatomy and physiology. Clin J Am Soc Nephrol. 2008;3(Supplement 3):S131-S9.

17. Tran NT, Kim YK, Kim SY, Lee MH, Lee KB. Comparative Osteogenesis and Degradation Behavior of Magnesium Implant in Epiphysis and Diaphysis of the Long Bone in the Rat Model. Materials. 2022;15(16): 5630.

18. Staiger MP, Pietak AM, Huadmai J, Dias G. Magnesium and its alloys as orthopedic biomaterials: a review. Biomaterials. 2006;27(9):1728-34.

19. Li L, Zhang M, Li Y, Zhao J, Qin L, Lai Y. Corrosion and biocompatibility improvement of magnesium-based alloys as bone implant materials: a review.

Regen Biomater. 2017;4(2):129-37.

20. Bellucci D, Mazzilli A, Martelli A, Mecca FG, Bonacorsi S, Lofaro FD, et al. Enrichment of strontium and magnesium improves the physical, mechanical and biological properties of bioactive glasses undergoing thermal treatments: New cues for biomedical applications. Ceram Int. 2024;50(24): 52819-52837

21. Li Y, Zhou J, Pavanram P, Leeflang MA, Fockaert LI, Pouran B, et al. Additively manufactured biode-gradable porous magnesium. Acta Biomate. 2018;67: 378-92.

22. Song Y, Shan D, Chen R, Zhang F, Han E-H. Biodegradable behaviors of AZ31 magnesium alloy in simulated body fluid. Mater Sci Eng C. 2009;29(3): 1039-45.

23. Kuwahara H, Al-Abdullat Y, Mazaki N, Tsutsumi S, Aizawa T. Precipitation of magnesium apatite on pure magnesium surface during immersing in Hank's solution. Mater Trans.2001;42(7):1317-21.

24. Liu YK, Lu QZ, Pei R, Ji HJ, Zhou GS, Zhao XL, et al. The effect of extracellular calcium and inorganic phosphate on the growth and osteogenic differentiation of mesenchymal stem cells *In vitro*: implication for bone tissue engineering. Biomed Mater. 2009;4(2):025004.

25. Wang Y, Geng Z, Huang Y, Jia Z, Cui Z, Li Z, et al. Unraveling the osteogenesis of magnesium by the activity of osteoblasts *In vitro*. J Mater Chem B. 2018;6(41):6615-21.

26. Maradze D, Musson D, Zheng Y, Cornish J, Lewis M, Liu Y. High Magnesium Corrosion Rate has an Effect on Osteoclast and Mesenchymal Stem Cell Role During Bone Remodelling. Sci Rep. 2018;8(1):10003.

27. Opal SM, DePalo VA. Anti-Inflammatory Cytokines. Chest. 2000;117(4):1162-72.

28. Sun Q, Zhou Y, Zhang A, Wu J, Tan L, Guo S. The immunomodulatory effects and mechanisms of magnesium-containing implants in bone regeneration: A review. J Magnes Alloys. 2024;12(7):2695-710.

29. Wang T, Ma X, Gong B, Zhu C, Xue P, Guo L, et al. Bio-inspired Ti3C2Tx MXene composite coating for enhancing corrosion resistance of aluminum alloy in acidic environments. J Colloid Interface Sci. 2024; 658:865-78.

30. Väänänen HK, Laitala-Leinonen T. Osteoclast lineage and function. Arch Biochem Biophys. 2008;473(2): 132-8.

31. Wu L, Luthringer BJC, Feyerabend F, Schilling AF, Willumeit R. Effects of extracellular magnesium on the differentiation and function of human osteoclasts. Acta Biomater.2014;10(6):2843-54.

32. Kraus T, Fischerauer SF, Hänzi AC, Uggowitzer PJ, Löffler JF, Weinberg AM. Magnesium alloys for temporary implants in osteosynthesis: in vivo studies of their degradation and interaction with bone. Acta Biomater.2012;8(3):1230-8.

33. Yamamoto A, Kikuta A. Development of a Model System for Gas Cavity Formation Behavior of Magnesium Alloy Implantation. ACS Biomater Sci Eng.2022;8(6):2437-44.

34. Park RS, Kim YK, Lee SJ, Jang YS, Park IIS, Yun YH, et al. Corrosion behavior and cytotoxicity of Mg-35Zn-3Ca alloy for surface modified biodegradable implant material. J Biomed Mater Res B Appl Biomater. 2012;100B(4):911-23.

Research Article

Effects of biocorrosion of biodegradable magnesium on the implantation environment

Yu-Kyoung Kim, Seo-Young Kim, Min-Ho Lee, Yong-Seok Jang[*]

*Department of Dental Biomaterials, Institute of Biodegradable Materials,
School of Dentistry, Jeonbuk National University, Jeonju, Republic of Korea*

Biodegradable magnesium metal has gained attention as temporary implants for dentistry and orthopedics due to their biodegradability and biocompatibility. This study analyzed the effects of magnesium corrosion and ion release on the cellular environment. The effects of Mg ion concentration and pH changes in the culture medium on osteoblast proliferation, differentiation, and macrophages inflammatory response were evaluated. Osteoblast alkaline phosphatase activity increased, and cell viability was high in an alkaline environment (pH 8–8.5). However, in co-cultures of osteoblasts and macrophages, secretion of inflammatory cytokines (TNF-α and IL-1β) and osteoclast differentiation were promoted at pH levels over and under 7. This suggests that local alkalinization due to magnesium corrosion can stimulate inflammation and bone resorption. In *in vivo* study, gas formation and tissue changes were observed after magnesium insertion into intermuscular and subdermal regions. In the intermuscular region, a large amount of gas was present for the first 3 weeks but gradually decreased after 6 weeks, disappearing after 12 weeks. Faster gas absorption and tissue recovery occurred in subdermal tissue. Gas formation and tissue changes due to corrosion promote inflammatory responses and interactions between cells, affecting the long-term stability of magnesium implants.

Keywords : Magnesium, biodegradability, cellular environment